

March 2003

The Quark-Meson Model and the Phase Diagram of Two-Flavour QCD

N. Tetradis

Department of Physics, University of Athens, Zographou 157 71, Greece

Abstract

We study the qualitative features of the QCD phase diagram in the context of the linear quark-meson model with two flavours, using the exact renormalization group. We identify the universality classes of the second-order phase transitions and calculate critical exponents. In the absence of explicit chiral-symmetry breaking through the current quark masses, we discuss in detail the tricritical point and demonstrate that it is linked to the Gaussian fixed point. In its vicinity we study the universal crossover between the Gaussian and $O(4)$ fixed points, and the weak first-order phase transitions. In the presence of explicit chiral-symmetry breaking, we study in detail the critical endpoint of the line of first-order phase transitions. We demonstrate the decoupling of pion fluctuations and identify the Ising universality class as the relevant one for the second-order phase transition.

1 Introduction

The phase diagram of QCD at non-zero temperature and baryon density has been the subject of many studies during the last years. (For a review see ref. [1].) Parts of this phase diagram may be observable through the heavy-ion collision experiments at RHIC and LHC. In particular, the conditions for the transition from the hadronic phase to the quark gluon plasma at high temperature and relatively low baryon density could be realized at these experiments. It is, therefore, desirable to connect the various regions of the phase diagram with clear experimental signatures. The most prominent feature of the phase diagram in this respect is the critical endpoint that marks the end of the line of first-order phase transitions. Its exact location and the size of the critical region around it determine its relevance for the experiments. There exist several analytical studies of the phase diagram near the critical endpoint. They employ effective theories of QCD [2]–[10], as analytical calculations in the context of the exact theory are very difficult. Lattice simulations are a source of precise information for full QCD. Recent studies [11, 12, 13] have overcome the difficulties associated with simulating systems with non-zero chemical potential, even though the continuum limit or realistic quark masses have not been reached yet.

The investigation of large regions of the phase diagram, so as to capture the interplay between critical and non-critical behaviour around the endpoint, seems more accessible to analytical methods. The description of the critical region makes the use of the renormalization group necessary. The study of first-order phase transitions is easier within the Wilsonian (or exact) formulation [14]. For these reasons, we would like to derive the QCD phase diagram employing an analytical approach that incorporates the exact renormalization group. A lot of work has been done on this method in recent years [15]. We shall use the effective average action [16], that results by integrating out (quantum or thermal) fluctuations above a certain cutoff k . Its dependence on k is given by an exact evolution equation [17, 18], while it becomes the effective action for $k = 0$. It can be used in order to describe very efficiently the universal and non-universal aspects of second-order phase transitions, as well as strong or weak first-order phase transitions [19].

We shall not study the full QCD for several reasons: the various formulations of the exact renormalization group for gauge theories [20]–[23] have not been complemented yet with efficient approximations for practical calculations. Moreover, a treatment of the exact evolution equation that could capture the effects of the confining region of QCD has not been developed.

We shall work within an effective theory of QCD, the linear quark-meson model, that uses as fundamental degrees of freedom mesons coupled to quarks. If only the two lightest quarks are taken into account the model is similar to the σ -model of Gell-Mann and Levy [24], with the nucleons replaced by quarks. The Lagrangian involves four scalar fields (the σ -field and the three pions π_i) arranged in a 2×2 matrix Φ , as well as the u and d quarks in a doublet. It is invariant under a global $SU(2)_L \times SU(2)_R$ symmetry acting on Φ and the quark doublet. If the σ -field develops an expectation value the symmetry is broken down to $SU(2)_{L+R}$. The model is very useful for studying the spontaneous

breaking of chiral symmetry, using Φ as the order parameter. The explicit breaking of this symmetry through the quark masses can also be incorporated. It corresponds to the interaction with an external source through a term $-j\sigma$ in the Lagrangian.

The linear quark-meson model has been studied for a general number of flavours and its phenomenological viability has been established [25]. Its formulation for non-zero temperature and quark chemical potential has also been developed [26, 27]. In particular, it has been found that, for two massless quark flavours, the model predicts a second-order phase transition for increasing temperature and zero chemical potential, and a first-order one for increasing chemical potential and zero temperature. It is likely, therefore, that the expected phase diagram of QCD for small chemical potential can be reproduced correctly within this effective theory. We point out, however, that the study of the colour superconducting or colour-flavour locked phases [1] requires the introduction of degrees of freedom that correspond to diquark condensates.

In this work we shall study the phase diagram of the quark-meson model. We consider only the case of two flavours as the basic structure appears already within this approximation. The generalization to three flavours is straightforward, even though the degree of complexity increases significantly. We do not consider realistic values for the various parameters of the Lagrangian. The reason is that the treatment of the exact evolution equation becomes complicated for the realistic values and little analytical progress can be made. Instead, one has to rely heavily on numerics that obscures the basic features of the problem. The consideration of parameter values consistent with the phenomenology is an obvious subject for future studies.

Despite the above limitations, our work includes several important elements: The infrared region is treated correctly through the renormalization group. The fixed point structure can be obtained in detail. The universal behaviour near the critical points can be distinguished from the non-universal aspects. The various universality classes can be identified and the crossover behaviour from one to the other can be studied.

In section 2 we discuss the phase diagram in the context of mean field theory in order to determine the main features we expect to appear. In section 3 we present the main ingredients of the model we are considering. In section 4 we derive the evolution equation that describes the dependence of the potential on a scale k that acts as an infrared cutoff. In section 5 we cast this equation in a form that has no explicit dependence on k and facilitates the identification of fixed points. In section 6 we derive the initial conditions for the solution of the evolution equation at energy scales below the temperature, where the evolution becomes effectively three-dimensional. In section 7 we use the formalism in order to discuss the phase diagram in the absence of explicit chiral symmetry breaking (zero current quark masses). In section 8 we discuss the phase diagram in the presence of explicit chiral symmetry breaking. In section 9 we summarize our findings and outline the directions of future research.

2 Mean field theory

In order to obtain some intuition on the form of the phase diagram, it is instructive to discuss a simple model in the mean-field approximation. The Lagrangian contains standard kinetic terms for the fields σ , π_i ($i = 1, 2, 3$), and the potential

$$U(\rho) = m^2\rho + \frac{1}{2}\lambda\rho^2 + \frac{1}{3}\nu\rho^3, \quad (1)$$

with $\rho = (\sigma^2 + \pi_i\pi^i)/2$. The couplings m^2 , λ , ν are taken to be functions of two external parameters, which we denote by T and μ without having to be more specific at this stage. We assume that ν is always positive, so that the potential is bounded from below.

Let us consider first the case $\lambda > 0$. For $m^2 > 0$ the minimum of the potential is located at $\sigma = \pi_i = 0$ and the system is invariant under an $O(4)$ symmetry. For $m^2 < 0$ the minimum moves away from the origin. Without loss of generality we take it along the σ axis. The symmetry is broken down to $O(3)$. The π 's, which play the role of the Goldstone fields, become massless at the minimum. If $m^2(T, \mu)$ has a zero at a certain value $T = T_{cr}$, while $\lambda(T_{cr}, \mu) > 0$, the system undergoes a second-order phase transition at this point. The minimum of the potential behaves as $\sigma_0 \sim |T - T_{cr}|^{1/2}$ slightly below the critical temperature. The critical exponent β takes the mean field value $\beta = 1/2$.

Let us consider now the case $\lambda < 0$. It is easy to check that, as m^2 increases from negative to positive values (through an increase of T for example), the system undergoes a first-order phase transition. For $|\lambda|$ approaching zero the phase transition becomes progressively weaker: The discontinuity in the order parameter (the value of σ at the minimum) approaches zero. For $\lambda = 0$ the phase transition becomes second order. The minimum of the potential behaves as $\sigma_0 \sim |T - T_{cr}|^{1/4}$. The critical exponent β takes the value $\beta = 1/4$ for this particular point.

Let us assume now for simplicity that λ is a decreasing function of μ only, and has a zero at $\mu = \mu_*$. If we consider the phase transitions for increasing T and fixed μ we find a line of second-order phase transitions for $\mu < \mu_*$, and a line of first-order transitions for $\mu > \mu_*$. The two lines meet at the special point (T_*, μ_*) , where $T_* = T_{cr}$ for $\mu = \mu_*$. This point is characterized as a tricritical point.

If a source term $-j\sigma$ is added to the potential of eq. (1) the $O(4)$ symmetry is explicitly broken. The phase diagram is modified significantly even for small j . The second-order phase transitions, observed for $\lambda > 0$, disappear. The reason is that the minimum of the potential is always at a value $\sigma \neq 0$ that moves close to zero for increasing T . For small j the mass term at the minimum approaches zero at a value of T near what we defined as T_{cr} for $\lambda = 0$. However, no genuine phase transition appears. Instead we observe an analytical crossover.

The line of first-order transitions persists for $j \neq 0$. However, for increasing T the minimum jumps discontinuously between two non-zero values of σ and never becomes zero. The line ends at a new special point, whose nature can be examined by considering the σ -derivative of the potential $U(\rho)$ of eq. (1). For a first-order phase transition to occur, $\partial U/\partial\sigma$ must become equal to j for three non-zero values of σ . This requires

$\partial^2 U / \partial \sigma^2 = 0$ at two values of σ . The endpoint corresponds to the situation that all these values merge to one point. It can be checked that this requires $\lambda < 0$. At the minimum σ_* of the potential $\tilde{U}(\sigma; j) = U(\sigma, \pi_i = 0) - j\sigma$ at the critical endpoint, we have: $d\tilde{U}/d\sigma = d^2\tilde{U}/d\sigma^2 = d^3\tilde{U}/d\sigma^3 = 0$. Therefore, at the endpoint we expect a second-order phase transition for the deviation of σ from σ_* . As $\lambda \neq 0$, the critical exponent β takes the value $\beta = 1/2$. The π 's are massive, because $m_\pi^2 = \partial^2 U(\rho) / \partial \pi_i^2 = dU(\rho) / d\rho = j / \sigma_*$ at the critical endpoint.

The purpose of the following is to reconstruct the above picture in the context of the linear quark-meson model. We shall take into account the effect of fluctuations of the fields, so that the potential will have a more complicated form than the simple assumption of eq. (1). Moreover, the nature of the fixed points will differ from the predictions of mean field theory.

3 The model

We consider an effective action of the form [25, 26, 27]

$$\Gamma_k = \int_0^{1/T} dx^0 \int d^3x \left\{ i\bar{\psi}^a (\gamma^\mu \partial_\mu + \mu \gamma^0) \psi_a + h\bar{\psi}^a \left[\frac{1 + \gamma^5}{2} \Phi_a^b - \frac{1 - \gamma^5}{2} (\Phi^\dagger)_a^b \right] \psi_b + \partial_\mu \Phi_{ab}^* \partial^\mu \Phi^{ab} + U_k(\rho; \mu, T) - \frac{1}{2} (\Phi_{ab}^* j^{ab} + j_{ab}^* \Phi^{ab}) \right\}, \quad (2)$$

with $\rho = \text{Tr}(\Phi^\dagger \Phi)$. The field Φ includes the σ field and the three pion fields. It is parametrized as

$$\Phi = \frac{1}{2} (\sigma + i\vec{\pi} \cdot \vec{\tau}) \quad (3)$$

where τ_l ($l = 1, 2, 3$) denote the Pauli matrices. The fermionic field ψ^a includes two flavours ($a = 1, 2$) corresponding to the up and down quarks. The non-zero temperature effects are taken into account by restricting the time integration within the finite interval $[0, 1/T]$ in Euclidean space. The scalar (fermionic) fields obey periodic (anti-periodic) boundary conditions. We are also considering a non-zero chemical potential, associated to the quark number density $\psi_a^\dagger \psi^a$ that is proportional to the baryon number.

In the effective action we have omitted the wavefunction renormalization for both the scalar and fermionic fields. We have also neglected the scale dependence of the Yukawa coupling h . We take into account only the scale dependence of the potential U_k , which we assume to be a general function of ρ . Our approximation is consistent in two cases:

a) If the Yukawa coupling is small at an initial large momentum scale Λ , its subsequent evolution for $k < \Lambda$ is expected to be slow. The reason is that the leading contribution to $dh^2/d\ln k$ is $\sim h^2$ [27]. The same holds true for the wavefunction renormalizations [27]. The scalar field wavefunction renormalization receives an additional contribution through scalar field contributions. Typically this is small in three and four dimensions, as is obvious from the smallness of the anomalous dimension in the pure scalar theory.

2) If partial infrared fixed points exist in the evolution equations, all the above quantities take almost constant values. The wavefunction renormalizations can be set equal to 1 through the rescaling of the fields, while the Yukawa coupling becomes scale independent. This scenario is realized in the low energy regime of the quark-meson model in four dimensions, for realistic values of the quark and meson masses.

The last term in eq. (2) accounts for the explicit breaking of the chiral symmetry through the current quark masses. One expects $j \sim M = \text{diag}(m_u, m_d)$. We assume equal masses \hat{m} for the two light quarks so that $j^a_b \sim \hat{m}\delta^a_b$. The determination of the proportionality constant requires the embedding of the theory described by the action (2) in a more fundamental framework. For example, in refs. [27, 28, 29] it was calculated in terms of the energy scale k_Φ at which Φ can be introduced as a composite field in a theory of quarks (such as the Nambu–Jona-Lasinio model [30]). One obtains $j = 2Z_{\psi, k_\Phi} m_{k_\Phi}^2 M/h_{k_\Phi}$, with Z_{ψ, k_Φ} the fermion wavefunction renormalization, and $m_{k_\Phi}^2$ the positive mass term in the potential of Φ at the scale k_Φ . This mass term becomes negative at lower energy scales because of fermionic quantum fluctuations, and the chiral symmetry is spontaneously broken. In this work we set $Z_{\psi, k} = 1$ for all k and also neglect the running of h_k . For this reason it is not possible to express j in terms of fundamental quantities. However, j can be fixed through the low energy dynamics. The pion mass at the vacuum in the presence of explicit chiral symmetry breaking is proportional to the source term and can be used as input for its determination.

4 The evolution equation

The dependence of the effective action Γ_k on an infrared cutoff scale k is given by an exact flow equation [17], which for fermionic fields ψ (quarks) and bosonic fields Φ (mesons) reads

$$\frac{\partial}{\partial k} \Gamma_k[\psi, \Phi] = \frac{1}{2} \text{Tr}_B \left\{ \frac{\partial R_{kB}}{\partial k} \left(\Gamma_k^{(2)}[\psi, \Phi] + R_k \right)^{-1} \right\} - \text{Tr}_F \left\{ \frac{\partial R_{kF}}{\partial k} \left(\Gamma_k^{(2)}[\psi, \Phi] + R_k \right)^{-1} \right\}. \quad (4)$$

Here $\Gamma_k^{(2)}$ is the matrix of second functional derivatives of Γ_k with respect to both fermionic and bosonic field components. The first trace in the r.h.s. of (4) runs only over the bosonic degrees of freedom. It implies a momentum integration and a summation over flavor indices. The second trace runs over the fermionic degrees of freedom and contains in addition a summation over Dirac and color indices. The terms R_{kB} , R_{kF} are infrared cutoffs that have been introduced in order to eliminate contributions from fluctuations with momenta $q^2 \lesssim k^2$ in the momentum integrations.

The evolution equation for the scale dependent potential U_k has been computed in ref. [26] starting from eq. (4). In the approximation that we neglect the running of the Yukawa coupling it takes the simplified form:

$$\frac{\partial}{\partial k} U_k(\rho; T, \mu) = \frac{\partial}{\partial k} U_{kB}(\rho; T, \mu) + \frac{\partial}{\partial k} U_{kF}(\rho; T, \mu), \quad (5)$$

where

$$\begin{aligned} \frac{\partial}{\partial k} U_{kB}(\rho; T, \mu) &= \frac{1}{2} T \sum_n \int_{-\infty}^{\infty} \frac{d^3 \vec{q}}{(2\pi)^3} \frac{\partial R_{kB}(\vec{q}^2 + 4n^2 \pi^2 T^2)}{\partial k} \left[\frac{3}{P_k(\vec{q}^2 + 4n^2 \pi^2 T^2) + U'_k(\rho; T, \mu)} \right. \\ &\quad \left. + \frac{1}{P_k(\vec{q}^2 + 4n^2 \pi^2 T^2) + U'_k(\rho; T, \mu) + 2\rho U''_k(\rho; T, \mu)} \right] \end{aligned} \quad (6)$$

and

$$\frac{\partial}{\partial k} U_{kF}(\rho; T, \mu) = \frac{\partial}{\partial k} \left[{}^4V_{kF}(\rho) + {}^3V_{kF}(\rho; T, \mu) + {}^3V_{kF}(\rho; T, -\mu) \right] \quad (7)$$

$${}^4V_{kF}(\rho) = -8N_c \frac{1}{2} \int_{-\infty}^{\infty} \frac{d^4 q}{(2\pi)^4} \theta(\Lambda^2 - q^2) \ln(q^2 + k^2 + h^2 \rho/2) \quad (8)$$

$${}^3V_{kF}(\rho; T, \mu) = -4N_c T \int_{-\infty}^{\infty} \frac{d^3 \vec{q}}{(2\pi)^3} \ln \left(1 + \exp \left[-\frac{1}{T} \left(\sqrt{\vec{q}^2 + k^2 + h^2 \rho/2} - \mu \right) \right] \right) \quad (9)$$

Here $\rho = \text{Tr}(\Phi^\dagger \Phi) = (\sigma^2 + \vec{\pi}^2)/2$ and $N_c = 3$ denotes the number of colours.

The two terms in the r.h.s. of eq. (5) correspond to the contributions from scalar and fermionic fluctuations. The scalar term, given by eq. (6), includes the contributions from the radial mode (the σ field) and the three Godstone modes (the pions). The parametrization in terms of ρ makes apparent the $O(4)$ symmetry characterizing the mesonic sector in the two-flavour case. The meson mass terms are $U'_k + 2\rho U''_k$, U'_k , where primes denote derivatives of the potential with respect to ρ . If the chiral symmetry is broken by an expectation value for the σ field, the mass terms become $m_\sigma^2 = \partial^2 U_k / \partial \sigma^2$, $m_\pi^2 = (1/\sigma) \partial U_k / \partial \sigma$, as expected.

The scale dependent propagators also contain the momentum dependent part $P_k = q^2 + R_{kB}(q^2)$. The term

$$R_{kB}(q^2) = \frac{q^2 e^{-q^2/k^2}}{1 - e^{-q^2/k^2}} \quad (10)$$

acts as an effective infrared cutoff in the loop integrations that determine the effective potential. The scale dependence of U_{kB} originates in this cutoff, as is apparent from the k -derivative of R_{kB} in eq. (6). The periodic conditions imposed on the scalar fields for non-zero temperature result in the replacement of the integration over q^0 by a sum over the discrete Matsubara frequencies. The chemical potential μ affects U_{kB} only through the contribution of the fermionic part U_{kF} to the mass terms.

The fermionic contribution U_{kF} has a simple interpretation within our approximate treatment. It consists of three parts: The term ${}^4V_{kF}(\rho)$ originates in the quantum fluctuations of the fermionic fields, for which a mass-like infrared cutoff k^2 has been introduced. This type of cutoff does not provide automatic ultraviolet regularization. This is achieved through the modification of the cutoff by an additional θ -function [26]. The number of degrees of freedom is $2(\text{flavour}) \times 2(\text{spin}) \times 2(\text{particle-antiparticle}) \times N_c$ (colour). The term ${}^3V_{kF}(\rho; T, \mu)$ is the free energy of a non-interacting fermionic gas of temperature T and

chemical potential μ in the presence of the mass-like cutoff k^2 . The ultraviolet regularization has been omitted as we assume $\Lambda \gg T$. The number of degrees of freedom is $2(\text{flavour}) \times 2(\text{spin}) \times N_c$ (colour). The term ${}^3V_{kF}(\rho; T, -\mu)$ is the free energy of the anti-particles that have opposite chemical potential. We emphasize that the evolution of U_{kF} is derived starting from the exact flow equation for the effective action of the system. The truncation of eq. (2) and the additional assumptions of constant wavefunction renormalizations and Yukawa coupling lead to the intuitive form of eqs. (7)–(9). We also point out that the use of different cutoffs for the scalar and fermionic fields does not affect physical quantities, as the cutoffs are removed in the limit $k \rightarrow 0$.

5 Scaling form of the evolution equation

Rather than solving eq. (5), it is more convenient to solve the evolution equation for U'_k . This can be written in the form

$$\begin{aligned} \frac{\partial}{\partial k} U'_k(\rho; T, \mu) &= v_4 k (3U''_k + 2\rho U'''_k) L_1^4 \left((U'_k + 2\rho U''_k)/k^2; T \right) + 3v_4 k U''_k L_1^4 \left(U'_k/k^2; T \right) \\ &\quad + \frac{\partial^2}{\partial k \partial \rho} \left[{}^4V_{kF}(\rho) + {}^3V_{kF}(\rho; T, \mu) + {}^3V_{kF}(\rho; T, -\mu) \right], \end{aligned} \quad (11)$$

where, in general dimensions d ,

$$v_d^{-1} = 2^{d+1} \pi^{d/2} \Gamma \left(\frac{d}{2} \right). \quad (12)$$

The “threshold” functions L_1^4 are particular cases of

$$L_n^d(w; T) = -2nk^{2n-d+1} \pi^{-\frac{d}{2}+1} \Gamma \left(\frac{d}{2} \right) T \sum_m \int d^{d-1} \vec{q} \frac{\partial P_k}{\partial k} (P_k + w k^2)^{-(n+1)}, \quad (13)$$

where P_k is a function of $\vec{q}^2 + 4n^2\pi^2 T^2$, as we discussed earlier.

The functions $L_n^d(w; T)$ have been discussed extensively in refs. [31, 32, 18, 19]. Their basic properties can be established analytically. For $T \ll k$ the summation over discrete values of m in the expression (13) is equal to the integration over a continuous range of q^0 , up to exponentially small corrections. Therefore

$$L_n^d(w; T) = L_n^d(w, 0) \equiv L_n^d(w) \quad \text{for } T \ll k. \quad (14)$$

In the opposite limit $T \gg k$ the summation over m is dominated by the $m = 0$ contribution. This results in the simple expression

$$L_n^d(w; T) = \frac{v_{d-1}}{v_d} \frac{T}{k} L_n^{d-1}(w) \quad \text{for } T \gg k, \quad (15)$$

with v_d defined in eq. (12). The two regions of T/k in which $L_n^d(w; T)$ is given by the equations (14), (15) are connected by a small interval $T/\theta_2 < k < T/\theta_1$ with a

more complicated dependence on w and T . The transitions at $k = T/\theta_1$ and $k = T/\theta_2$ are sharp for an exponential cutoff, such as the one given by eq. (10). The functions $L_n^d(w)$ fall off for large values of w , following a power law. As a result they introduce a threshold behaviour for the contributions of massive modes to the evolution equations. These include L_n^d functions with the mass eigenvalues divided by k^2 as their arguments. When the running squared mass of a massive mode becomes much larger than the scale k^2 , the mode decouples the respective contribution vanishes. We evaluate the expressions for $L_n^d(w; T)$ numerically and use numerical fits for the solution of the evolution equations.

The fermionic contribution is expected to display a similar behaviour for decreasing k . It can be checked that the temperature-dependent term of eq. (9) evolves slowly for $k \lesssim T$ and obtains asymptotically a constant form. However, the k dependence disappears only as power law, instead of exponentially fast as for $L_n^d(w, T)$ above. The quantum contribution of eq. (8) has a strong dependence on the ultraviolet cutoff Λ that regulates the momentum integration. As a result, the quantity $\partial^2(^4V_{kF})/\partial k \partial \rho$ displays a logarithmic dependence on Λ . The above shortcomings are connected to the use of a mass-like cutoff for the fermionic sector, instead of an exponential cutoff as for the bosons. A mass like cutoff is the simplest choice that preserves the Lorentz structure of the kinetic term of free fermions for non-zero chemical potential, so as to make practical calculations feasible [26]. A more ingenious, and more complicated, form is required in order to preserve the correct Lorentz structure and guarantee exponential decoupling of the temperature effects for fermions at low energy scales.

In this work we are not interested in the details of fermion decoupling. For this reason we follow a different approach. We assume that at a sufficiently low scale $k \lesssim T$ the fermionic contributions to the evolution equation decouple. This is the expected behaviour, as the lowest Matsubara frequency is πT for the fermions and no zero mode exists. The result of the integration of the fermionic modes is a contribution equal to the perturbative one-loop term for the potential. It is clear that this assumption is consistent with the form of the terms of eqs. (8), (9) for $k = 0$. It is expected to be correct for small Yukawa coupling h .

We concentrate on the behaviour of the evolution equation (11) for $k \lesssim T$, in which, as we explained above, two important simplifications occur:

- a) The ‘‘threshold’’ functions are approximated very well by $L_1^4(w, T) = (4T/k)L_1^3(w)$.
- b) The fermions have decoupled because of their thermal masses.

We define the quantities

$${}^3U_k(\rho_3) = \frac{U_k(\rho; T, \mu)}{T} \quad (16)$$

$$\rho_3 = \frac{\rho}{T}, \quad (17)$$

and their dimensionless versions

$$u_k(\tilde{\rho}) = \frac{{}^3U_k(\rho_3)}{k^3} = \frac{U_k(\rho; T, \mu)}{k^3 T} \quad (18)$$

$$\tilde{\rho} = \frac{\rho_3}{k} = \frac{\rho}{kT}. \quad (19)$$

The evolution equation (11) can be rewritten in the scaling form [18]

$$\frac{\partial}{\partial t} u'_k(\tilde{\rho}) = -2u'_k + \tilde{\rho}u''_k + v_3(3u''_k + 2\tilde{\rho}u'''_k) L_1^3(u'_k + 2\tilde{\rho}u''_k) + 3v_3 u''_k L_1^3(u'_k), \quad (20)$$

with $t = \ln(k/M)$ and the primes denoting derivatives with respect to $\tilde{\rho}$. The energy scale M can be defined arbitrarily. The characteristic property of the above equation is that the scale k does not appear explicitly in it. This permits the search for fixed points, i.e. scale independent solutions. They are the solutions with $\partial u'_k/\partial t = 0$.

The evolution equation (20) has a form typical of a three-dimensional theory (dimensional reduction). This is expected, as only the fields with zero Matsubara frequencies (the scalar zero modes) are sufficiently light in order to contribute to the evolution.

6 Initial conditions for the evolution equation

The initial conditions for the solution of eq. (20) must be given at the scale $k_T = T/\theta_2$. Let us assume that at the large momentum scale Λ (where the effects associated with the temperature and chemical potential are negligible) the potential has the simple form

$$U_\Lambda(\rho) = U_\Lambda(\rho; 0, 0) = \frac{\lambda}{2}(\rho - \rho_{0\Lambda}), \quad (21)$$

with $\rho_{0\Lambda} < 0$. For small λ we can integrate the evolution equation (11) between the scales Λ and $k_T = T/\theta_2$, approximating the arguments of the threshold functions with zero and setting $U''_k = \lambda$, $U'''_k = 0$. These approximations account for the leading perturbative result and give [32, 33]

$$U'_{k_T}(\rho; T, \mu) \simeq \lambda \left[\rho - \left(\rho_{0\Lambda} - \frac{3}{16\pi^2} \Lambda^2 \right) - \frac{3}{4\pi^2} T^2 \left(\frac{\sqrt{\pi}}{\theta_2} - \frac{\pi^2}{3} \right) \right] + {}^4V'_{0F}(\rho) + {}^3V'_{0F}(\rho; T, \mu) + {}^3V'_{0F}(\rho; T, -\mu). \quad (22)$$

with ${}^4V_{0F}$, ${}^3V_{0F}$ given by eqs. (8), (9) with $k = 0$. We have assumed that the fermionic contributions have already decoupled at $k_T = T/\theta_2$ and are given by eq. (9) with $k = 0$. The term $\sim T^2$ results from the complicated form of $L_1^4(0; T)$ in the k -interval $[T/\theta_2, T/\theta_1]$ [33].

The $T = \mu = 0$ fermionic contribution (8) can be evaluated explicitly

$${}^4V'(\rho) = -N_c \frac{h^2}{8\pi^2} \Lambda^2 - N_c \frac{h^4}{16\pi^2} \rho \ln \left(\frac{\frac{h^2 \rho}{2\Lambda^2}}{1 + \frac{h^2 \rho}{2\Lambda^2}} \right). \quad (23)$$

We can cast eq. (22) in the form

$$U'_{k_T}(\rho; T, \mu) \simeq \lambda \left[\rho - \rho_{0R} - \frac{3}{4\pi^2} T^2 \left(\frac{\sqrt{\pi}}{\theta_2} - \frac{\pi^2}{3} \right) \right] + I_F(\rho; T, \mu) \quad (24)$$

with

$$\rho_{0R} = \rho_{0\Lambda} - \frac{3}{16\pi^2}\Lambda^2 + \frac{h^2}{\lambda} \frac{N_c}{8\pi^2}\Lambda^2 \quad (25)$$

$$I_F(\rho; T, \mu) = -N_c \frac{h^4}{16\pi^2} \rho \ln \left(\frac{\frac{h^2 \rho}{2\Lambda^2}}{1 + \frac{h^2 \rho}{2\Lambda^2}} \right) + {}^3V'_{0F}(\rho; T, \mu) + {}^3V'_{0F}(\rho; T, -\mu). \quad (26)$$

The $T = \mu = 0$ potential displays the spontaneous chiral symmetry breaking induced by the fermionic fluctuations. For sufficiently large Yukawa coupling h , even if $\rho_{0\Lambda}$ is negative (corresponding to a positive mass term), the renormalized value ρ_{0R} can become positive through the fermionic contribution in eq. (25).

At non-zero temperature, a consistency check for the initial condition (24) can be performed by integrating eq. (20) from $k = T/\theta_2$ to $k = 0$. Again we assume a small λ_R , set $U'_k = \lambda_R$, $U''_R = 0$ and take the arguments of the “threshold” functions equal to zero. In this way we obtain

$$U'_0(\rho; T, \mu) \simeq U'_{k_T}(\rho; T, \mu) + \frac{3}{4\pi^2} \frac{\sqrt{\pi}}{\theta_2} \lambda T^2 = \lambda \left[\rho - \rho_{0R} + 6 \frac{T^2}{24} \right] + I_F(\rho; T, \mu), \quad (27)$$

where we have used $L_1^3(0) = -\sqrt{\pi}$. This expression reproduces correctly the leading perturbative result [34] for the critical temperature. However, the assumption that the couplings remain small is not valid near the phase transition. Close to the critical temperature the fixed-point structure of the theory becomes important and the arguments of the “threshold” functions cannot be neglected.

Another ingredient that we have neglected in our considerations so far is the explicit chiral symmetry breaking term $\sim \sigma$, arising through the current quark masses. A term linear in σ does not appear explicitly in the evolution equations, as the flow equation (4) involves second functional derivatives of the action with respect to the fields. For this reason the linear term can be added directly to the potential at any scale.

7 The phase diagram for $j = 0$

Let us summarize the main points of the framework we have set up. Our theory is defined through the potential of eq. (21) at a scale $\Lambda \gg T$. In a realistic theory we can identify Λ with the energy scale k_Φ at which the mesonic fields σ , π_i can be introduced as composite fields in a theory of quarks. The renormalized potential for $k = 0$ and zero temperature and chemical potential is given by eqs. (24)–(26) with $T = \mu = 0$. These approximate expressions are correct if:

- a) h is small enough for its logarithmic running to be neglected. This requires corrections $\sim h^4/(4\pi^2)$ to be negligible relative to h^2 .
- b) λ is small enough for terms $\sim \lambda^2$ to be neglected. Notice, however, that corrections $\sim h^4/(4\pi^2)$ are not assumed to be small relative to λ . On the contrary, it is for the range $h^4/(4\pi^2) \sim \lambda$ that first-order phase transitions appear.

The explicit chiral symmetry breaking can be taken into account by adding a term $-j\sigma$ to the potential. The parameters ρ_{0R} , λ , j can be determined through the pion decay constant f_π and the masses m_σ , m_π of the σ and pion fields. The Yukawa coupling h can be determined through the constituent quark mass M_q .

At the scale $k_T = T/\theta_2$ the potential is given by eq. (22), with ${}^3V_{0F}$ given by eq. (9) for $k = 0$. The evolution of U_k for $k \leq k_T$ is given by eq. (20). The scalar modes with non-zero Matsubara frequencies, as well as the fermions, have completely decoupled. Only the fluctuations of the scalar zero modes contribute to the evolution of the potential. For this reason the theory is effectively three-dimensional at these low scales. For practical calculations we use $\theta_2 = 1$.

The fermionic contribution $I_F(\rho; T, \mu)$ to the initial condition for the potential, given by eq. (26), can be evaluated in certain limiting cases for small mass term $h^2\rho/2$. For $\mu = 0$ the standard high temperature expansion [34] gives

$$I_F(\rho; T, 0) = N_c \frac{h^2}{12} T^2 + N_c \frac{h^4}{16\pi^2} \rho \ln \left(\frac{\Lambda^2}{\alpha T^2} \right) + \mathcal{O}(h^6), \quad (28)$$

with $\alpha \simeq 8.5$. For $T = 0$ the Fermi-Dirac distribution becomes a step-function and we obtain

$$I_F(\rho; 0, \mu) = N_c \frac{h^2}{4\pi^2} \mu^2 + N_c \frac{h^4}{16\pi^2} \rho \ln \left(\frac{\Lambda^2}{\beta \mu^2} \right) + \mathcal{O}(h^6), \quad (29)$$

with $\beta \simeq 10.9$.

The terms $\sim h^4\rho$ in the r.h.s. of the above equations can change the sign of the tree-level term $\lambda\rho$ in the initial condition (24). The phase diagram expected for QCD is obtained if the total term $\sim \rho$ is positive near the phase transition for $T \neq 0$, $\mu = 0$ and negative for $T = 0$, $\mu \neq 0$. In our model we choose couplings such that this condition is satisfied. It has been checked explicitly [26, 27] that the realistic values of the parameters, consistent with low-energy QCD phenomenology, reproduce the correct order for the transitions for $T \neq 0$, $\mu = 0$ and $T = 0$, $\mu \neq 0$.

We define dimensionful quantities in terms of the parameter ρ_{0R} defined in eq. (25). Our analysis of the phase diagram will be carried out for a model with $\lambda = 0.1$, $h^2 = 2.3$, $\Lambda^2 = 1.8\rho_{0R}$.

7.1 The second-order phase transitions

We start by considering a system with zero chemical potential. In fig. 1 we display the solution of eq. (20), for a theory with $\mu = 0$, $T/\sqrt{\rho_{0R}} \simeq 0.407$. We start the evolution at a scale $k_T = T$ and move towards the infrared. The initial condition is given by eqs. (24), (26), and corresponds to a system in the broken phase. We observe that initially $u'_k(\tilde{\rho})$ is small, because of the smallness of the value of λ we chose. Subsequently the potential evolves (dashed lines), while its minimum $\tilde{\rho}_0$ remains non-zero. At a later stage the solution approaches an almost constant form (solid lines). This is the fixed point of the $O(4)$ universality class. At the last stages of the evolution (dotted lines) the minimum of the potential moves to the origin and $u'_k(0)$ becomes positive.

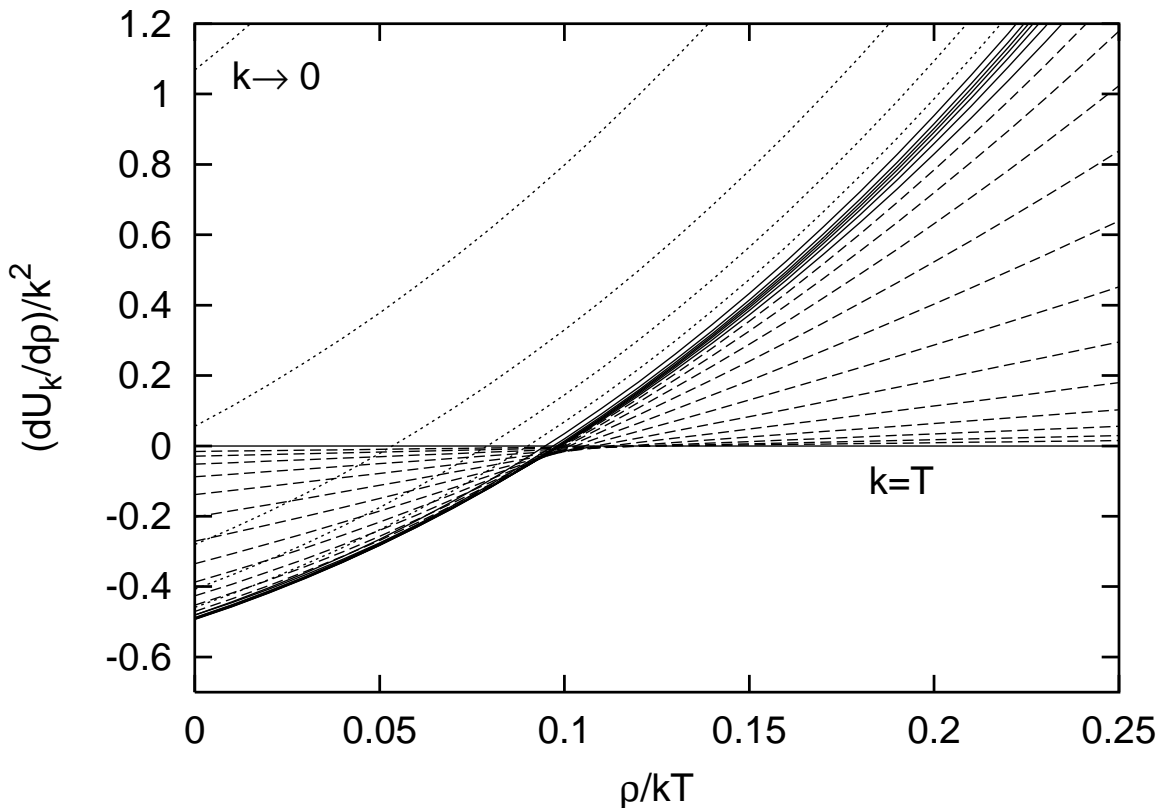


Figure 1: *The evolution of the rescaled potential for $\mu = 0$, $T/\sqrt{\rho_{0R}} \simeq 0.407$.*

For $k \rightarrow 0$, the rescaled mass term $u'_k(0)$ diverges so that $dU_k(0; T)/d\rho = k^2 du_k(0)/d\tilde{\rho}$ approaches a constant value. The system ends up in the symmetric phase. The renormalized mass term $m_R^2(T) = dU_0(0; T)/d\rho$ is very small in terms of the characteristic mass scale of the potential at $k = T$. The reason is that, during the “time” $t = \ln(k/\rho_{0R}^{1/2})$ the solution is close the fixed point, the quantity $u'_k(0)$ remains constant, so that $U'_k(0; T)$ scales $\sim k^2$. The longer the system spends near the fixed point, the smaller the final value of $m_R^2(T)$. The approach to the fixed point is controlled by one parameter, the temperature T . For the evolution displayed in fig. 1 the temperature is slightly larger than the critical value T_{cr} that separates the symmetric from the broken phase. For a value slightly smaller than the critical, the evolution would be similar to that in fig. 1, apart from the last stages. For $k \rightarrow 0$ the minimum $\tilde{\rho}_0$ of $u_k(\tilde{\rho})$ would diverge, so that the minimum ρ_0 of $U_k(\rho; T)$, given by $\rho_0(k, T) = \tilde{\rho}(k)kT$, would reach a constant very small value $\rho_{0R}(T)$. In this way, the system would end up in the broken phase. Examples of this behaviour can be found in the review [19] and references therein.

The fixed point of the $O(4)$ universality class is approached by fine-tuning only one relevant parameter, the temperature T of the system. The temperature effectively controls the mass term of the initial potential. The properties of the critical theory (the one for $T \simeq T_{cr}$) are determined only by the fixed point. The reason is that the system, after

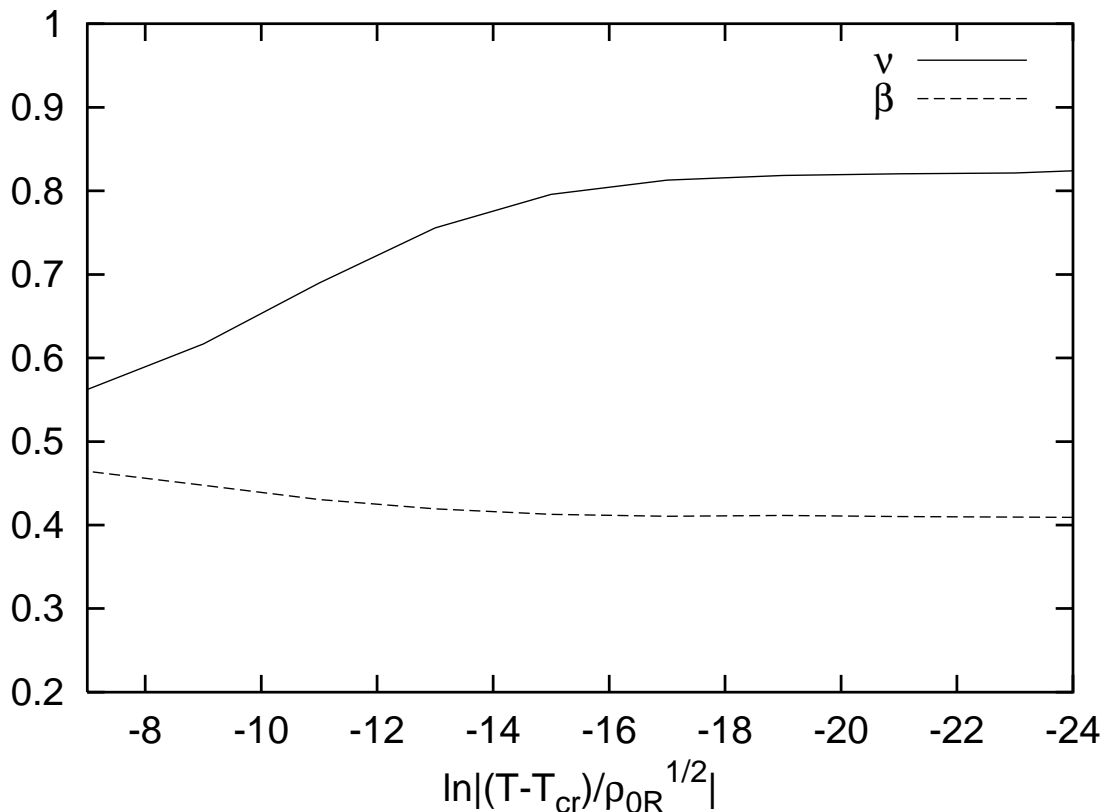


Figure 2: *The critical exponents ν and β as the critical temperature is approached.*

spending a significant part of the evolution near the fixed point, loses memory of the initial conditions. As a result, all physical quantities at the vacuum can be parametrized in terms of the deviation of T from T_{cr} . The dependence on $T - T_{cr}$ is not analytic. In particular, for the mass term and the expectation value we expect a behaviour that can be parametrized as

$$m_R^2(T) \sim |T - T_{cr}|^{2\nu} \quad (30)$$

$$\rho_{0R}(T) \sim |T - T_{cr}|^{2\beta}. \quad (31)$$

In fig. 2 we plot the effective values of the critical exponents ν , and β , extracted through the integration of the evolution equation for various values of T . We observe that the exponents become constant very close to the critical temperature, with values $\nu \simeq 0.82$, $\beta \simeq 0.41$. These are in reasonable agreement with the values determined through high precision calculations using alternative methods, or the effective average action taking into account the wavefunction renormalization: $\nu \simeq 0.74$, $\beta \simeq 0.38$ [19]. The discrepancy arises because we have neglected the wavefunction renormalization, effectively using $\eta = 0$ for the anomalous dimension of the field. The correct value of this quantity is $\eta \simeq 0.036$. Notice, however, that the scaling law $\beta = (1 + \eta)\nu/2$ is satisfied by our result.

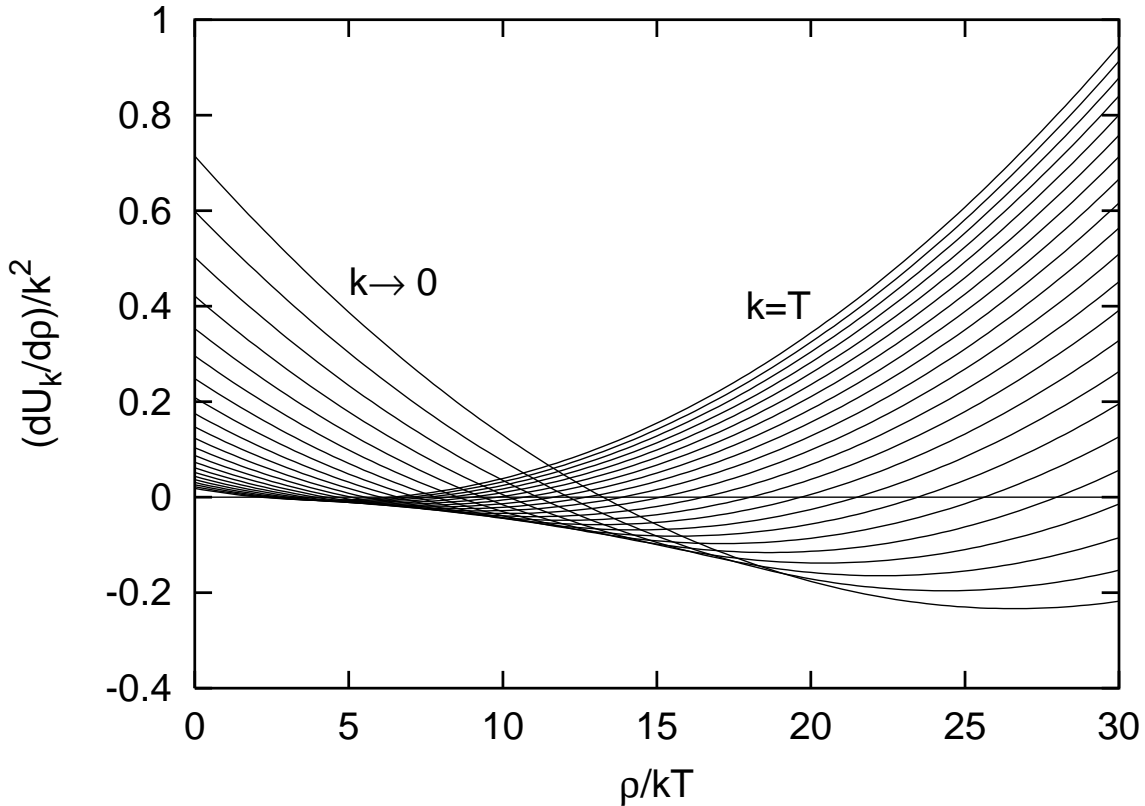


Figure 3: *The evolution of the rescaled potential for $\mu/\sqrt{\rho_{0R}} \simeq 0.735$, $T/\sqrt{\rho_{0R}} = 0.1$.*

7.2 The first-order phase transitions

We turn now to the region of first-order phase transitions, which are expected to take place for large values of the chemical potential. We consider a system with $\mu \simeq 0.735$, $T/\sqrt{\rho_{0R}} = 0.1$. In fig. 3 we display the evolution of $u'_k(\tilde{\rho})$ starting at $k = T$ and moving towards $k = 0$. This figure should be compared to fig. 1. The differences are significant. Already at $k = T$, there are two values of the order parameter $\tilde{\rho}$ for which u'_k vanishes. Moreover, $u'_k(0)$ is positive. This implies a potential with two minima (one located at the origin) and a maximum. During the evolution towards the infrared the system does not approach a fixed-point solution. For $k \rightarrow 0$, $u'_k(0)$ increases so that $U'_k(0; T, \mu)$ reaches a constant value. The point $\tilde{\rho}_0$ where the second minimum of u_k is located diverges also, so that the second minimum ρ_0 of U_k approaches a constant value.

The behaviour of $U_k(\rho; T, \mu)$ is displayed in fig. 4. We observe the two minima, and the curvature of the potential around them that determines the mass terms, settling down at constant values. The minimum at the origin is slightly deeper than the one at non-zero ρ , indicating that the temperature is slightly larger than the critical one. The barrier separating the two minima remains scale dependent even after the minima have become scale independent to a good approximation. This is a general feature of the solutions near first-order phase transitions, which is related to the issue of the convexity of the

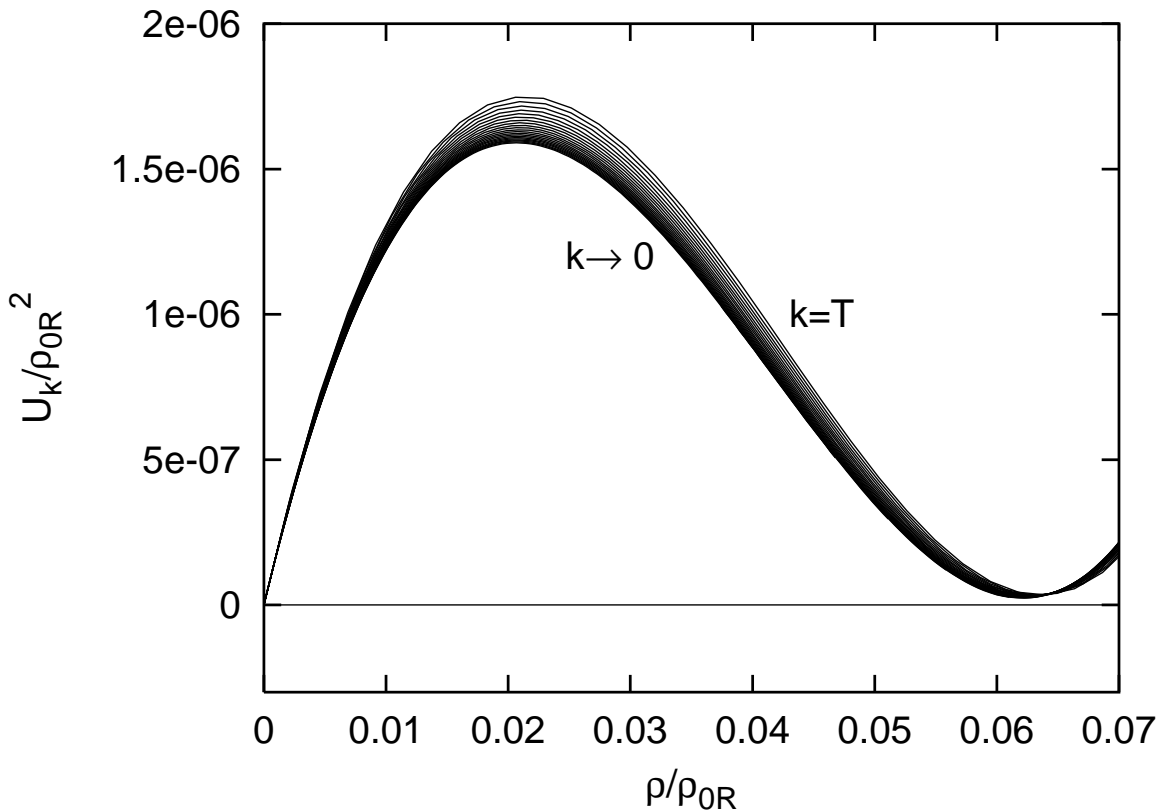


Figure 4: *The evolution of the potential for $\mu/\sqrt{\rho_{0R}} \simeq 0.735$, $T/\sqrt{\rho_{0R}} = 0.1$.*

effective potential [31, 19]. As the scale-dependent potential U_k approaches the effective potential for $k \rightarrow 0$, the barrier should disappear, giving its place to the standard Maxwell construction. This is a general property of the solutions of the evolution equation [31, 19], which can be established analytically. However, the numerical integration of the evolution equation in this regime is difficult because of the presence of a pole in the threshold function. For this reason, in fig. 4 we have stopped the evolution at a non-zero value of k , such that the minima are stabilized, even though the barrier has not disappeared yet. An example of a more elaborate numerical integration that displays the approach to convexity for $k \rightarrow 0$ is presented in ref. [19]. The calculation of bubble-nucleation rates during a first-order phase transition is performed at non-zero values of k . The physical value of the nucleation rate is independent of the choice of k at which the calculation is carried out [35].

7.3 The tricritical point

The second-order phase transitions, discussed in subsection 7.1, form a line on the phase diagram, which starts at $\mu = 0$ and continues towards non-zero values of μ . Similarly, the first-order phase transitions, discussed in subsection 7.2, form another line that starts at

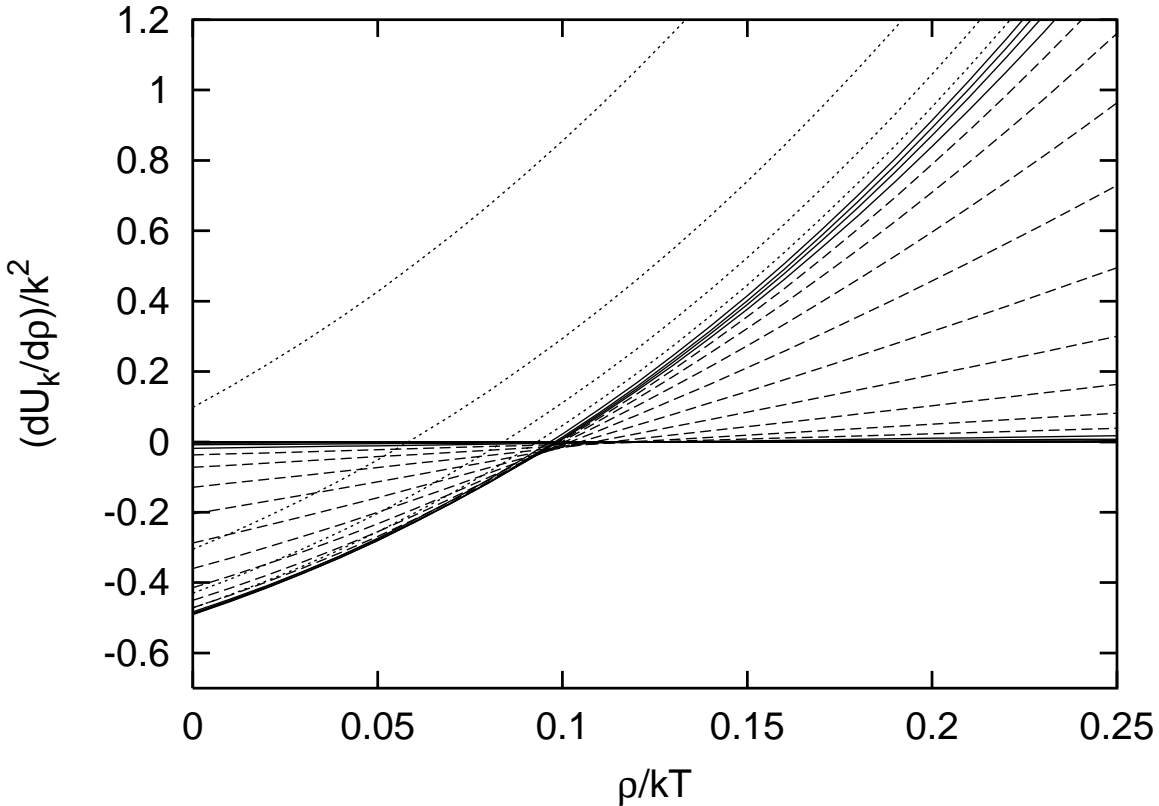


Figure 5: *The evolution of the rescaled potential for $\mu/\sqrt{\rho_{0R}} = 0.718$, $T/\sqrt{\rho_{0R}} \simeq 0.130$.*

$T = 0$ and continues towards non-zero values of T . These two lines are expected to meet at a point on the (T, μ) plane, characterized as the tricritical point. Near it the first-order transitions are very weak (the discontinuity in ρ approaches zero) and eventually become second order.

In fig. 5 we display the evolution of $u'_k(\tilde{\rho})$ for $\mu/\sqrt{\rho_{0R}} = 0.718$, $T/\sqrt{\rho_{0R}} \simeq 0.130$. This figure is very similar to fig. 1. The potential evolves towards the $O(4)$ fixed point, where it becomes stationary for a while. Eventually it moves away from the fixed point and settles down in the symmetric phase.

The significant difference between the two figures concerns the initial stage of the evolution. In fig. 1 this is rather short, as the potential moves quickly away from its initial form and approaches the fixed point. In fig. 5 the initial stage is much longer, as can be deduced from the accumulation of curves on the horizontal axis. In fact, two fixed points are apparent in fig. 5: the one characterizing the $O(4)$ universality class, and the Gaussian fixed point which corresponds to $u'_k(\tilde{\rho}) = 0$. The system starts very close to the Gaussian fixed point. This is unstable, so that eventually the system approaches the $O(4)$ fixed point. In order to start near the Gaussian fixed point, two relevant parameters must be fine-tuned: the temperature and the chemical potential. They control the mass term (the term $\sim \rho$) and the quartic coupling (the term $\sim \rho^2$) of the initial potential. In

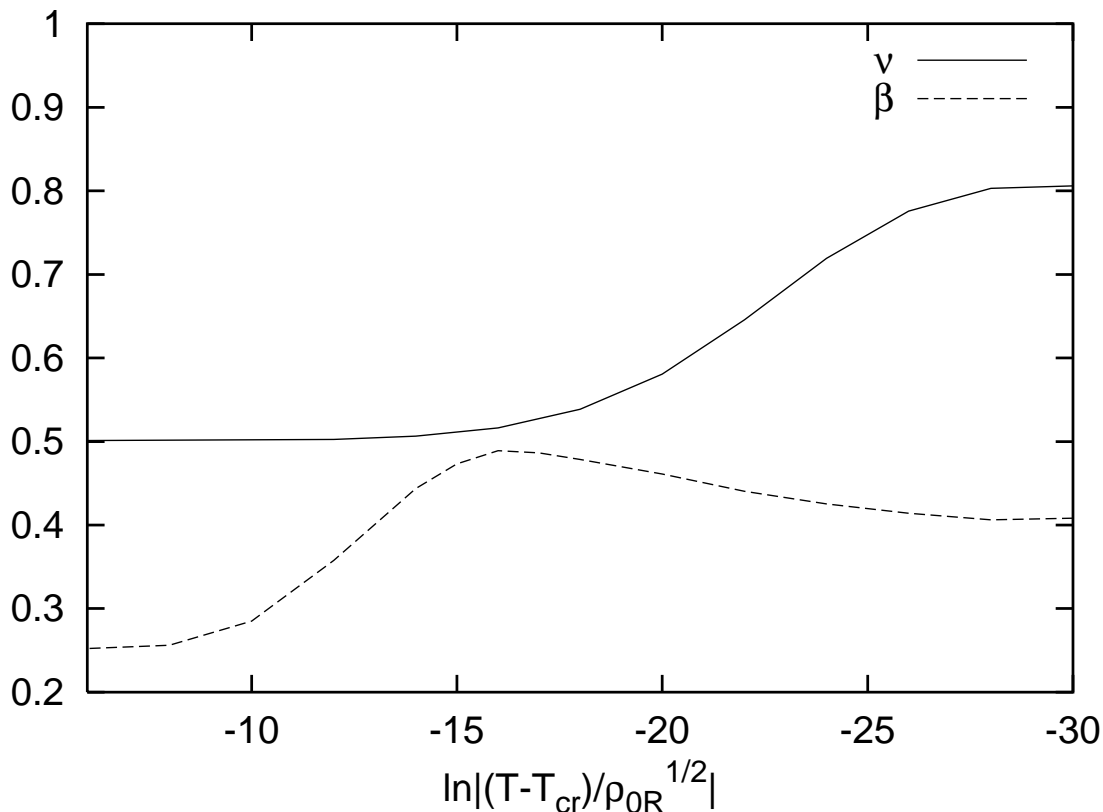


Figure 6: *The critical exponents ν and β as the critical temperature is approached near the tricritical point.*

particular, the initial values of these two terms are very close to zero, so that the term $\sim \rho^3$ (in an expansion of $U_{kT}(\rho)$ around the origin) is important.

These findings are in very good agreement with the discussion of section 2, which was based on mean field theory. The reason is that the Gaussian fixed point results in mean-field behaviour, as the effect of fluctuations is negligible because of the smallness of the couplings. Our results indicate that the tricritical point must be connected with the Gaussian fixed point of fig. 5. The number of relevant parameters is correctly predicted to be 2.

The effective critical exponents ν , β can be computed from eqs. (30), (31), similarly to subsection 7.1, by keeping μ fixed and varying T . The results are depicted in fig. 6. We observe that for $|T - T_{cr}|/\sqrt{\rho_{0R}} = \exp(-5) - \exp(-8)$ they take the values $\beta = 0.25$, $\nu = 0.5$. These are the mean-field predictions that we derived in section 2. For this range of temperatures the potential never approaches the $O(4)$ fixed point. It stays close to the Gaussian one, before moving directly towards the broken or the symmetric phase. For temperatures closer to T_{cr} , the system feels the attraction of the $O(4)$ fixed point. For T very close to T_{cr} the potential spends a large part of its evolution near this fixed point. As a result it loses memory of its initial form near the Gaussian fixed point. The critical

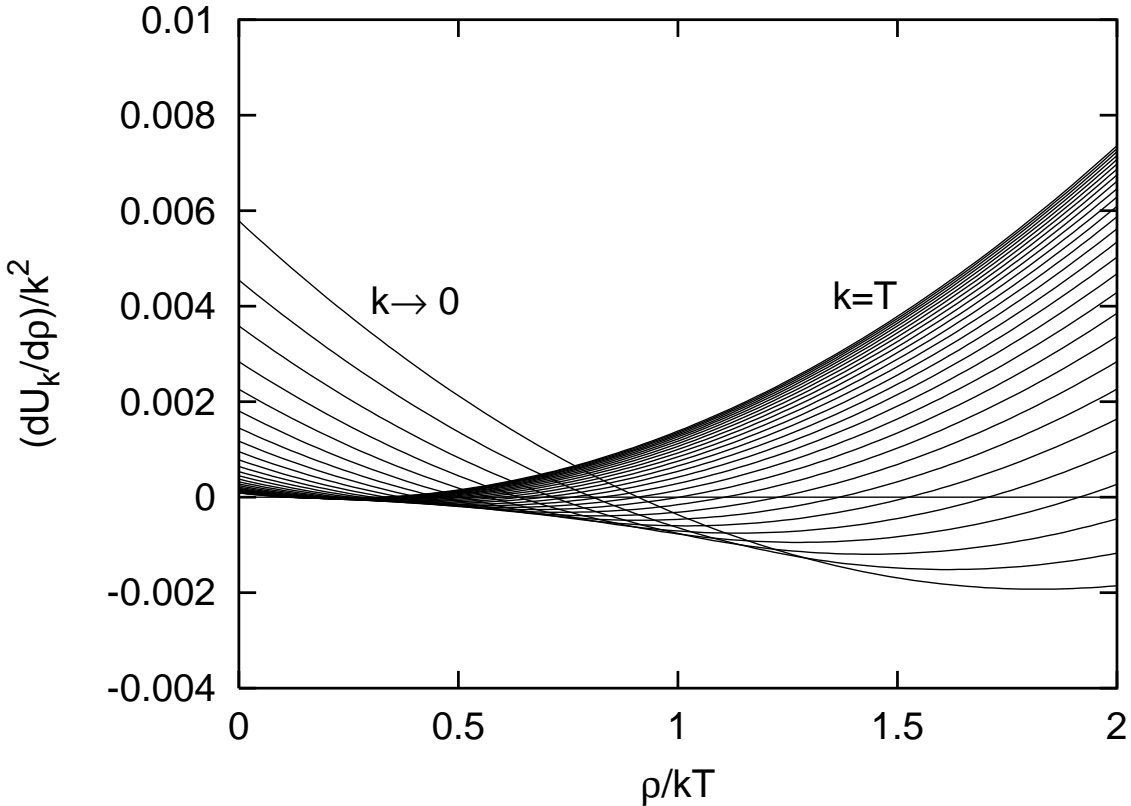


Figure 7: *The evolution of the rescaled potential for $\mu/\sqrt{\rho_{0R}} = 0.719$, $T/\sqrt{\rho_{0R}} \simeq 0.128$.*

exponents take the values characteristic of the $O(4)$ universality class.

The curves in fig. 6 between $|T - T_{cr}|/\sqrt{\rho_{0R}} = \exp(-9)$ and $|T - T_{cr}|/\sqrt{\rho_{0R}} = \exp(-30)$ are typical examples of crossover curves. They describe the variation of universal quantities, such as the critical exponents, as the relative influence of two fixed points changes.

We can confirm our identification of the tricritical point by studying the first-order phase transitions near the Gaussian fixed point. In fig. 7 we display the evolution of $u'_k(\tilde{\rho})$ for a theory with $\mu/\sqrt{\rho_{0R}} = 0.719$, $T/\sqrt{\rho_{0R}} \simeq 0.128$. The slight increase of the value of the chemical potential relative to fig. 5 modifies drastically the evolution. The potential stays very close to the Gaussian fixed point for a long “time” $t = \ln(k/\rho_{0R}^{1/2})$, but eventually moves away from it. (Notice the difference by a factor 100 of the scale of the vertical axis between figs. 3 and 7.) Its form is characteristic of a first-order phase transition as we discussed in detail in subsection 7.2. However, the transition is very weak, as the discontinuity in the order parameter is orders of magnitude smaller than ρ_{0R} .

The tricritical point is located on the plane $(\mu/\sqrt{\rho_{0R}}, T/\sqrt{\rho_{0R}})$ in the region between the points $(0.718, 0.130)$ and $(0.719, 0.128)$. For the critical values of μ and T_{cr} the solution of the evolution equation stays close to the Gaussian fixed point for an infinitely long “time” t . As a result the critical behaviour is determined completely by mean-field

theory. For example, the critical exponent β stays equal to 0.25 arbitrarily close to the critical temperature.

8 The phase diagram for $j \neq 0$

8.1 The analytical crossover and the first-order phase transitions

The effect of a source term $-j\sigma$ on a second-order phase transition has been studied extensively in the statistical physics and field theory literature. It is well known that the phase transition disappears and is replaced by an analytical crossover. No singularities appear in the physical quantities. Instead these are described by smooth functions connecting the two “phases”. The reason can be understood by considering the potential for a constant value of μ , corresponding to the part of the phase diagram where a second-order phase transition is expected for $j = 0$. The vacuum of the theory is determined by the relation $\partial U_0/\partial\sigma = j$. For $j \neq 0$ the vacuum is located away from the origin for all values of T . If we take σ as the order parameter, no signal of a phase transition exists. Moreover, both the σ -field and the pions are massive at the vacuum. This implies that no significant fluctuations exist in the deep infrared, as all fields decouple at sufficiently low energy scales. Consequently, no singularities are expected in physical quantities.

For very small j , the influence of the fixed point leads to a universal form of the potential in the critical region. It is convenient to define the quantity $x = \delta T/\sigma^{1/\beta}$, with $\delta T = T - T_{cr}$ and β a critical exponent. The potential can be expressed as

$$\frac{1}{\sigma^\delta} \frac{\partial U_0}{\partial\sigma} = f(x), \quad (32)$$

with δ another critical exponent and $\partial U_0/\partial\sigma = j$ [36]. The form of the function $f(x)$, characterized as the universal equation of state, is completely specified by the universality class. For small j , the temperature dependence of the σ -field and pion masses near the critical temperature can be extracted from eq. (32) [37].

We shall not determine the equation of state of the $O(4)$ universality class here, as it has been calculated in ref. [27]. There, it is also demonstrated how the interplay between universal and non-universal behaviour can be described efficiently by the effective average action. Even though the study of ref. [27] is carried out for $\mu = 0$, it displays all the characteristic features associated with theories in the small- μ region of the phase diagram.

The first-order phase transitions for large μ that we discussed in subsection 7.2 are not affected significantly by the presence of a source term $-j\sigma$. The minimum at the origin moves to a non-zero value of σ , as in the case of second-order phase transitions. The linear term also affects the relative depth of the two minima of the potential and changes the value of the critical temperature. The most characteristic feature of the phase diagram for $j \neq 0$ is the presence of a critical endpoint that marks the end of the line of first-order phase transitions. At this point a second-order phase transition is expected

to take place. In the following subsection we discuss in detail the nature of the endpoint and determine the relevant universality class.

8.2 The critical endpoint

In order to discuss the critical endpoint we need to adapt our formalism to the situation of explicit symmetry breaking through the addition of the source term $-j\sigma$ to the potential. In particular, we have to define an appropriate order parameter that can describe the second-order phase transition. For this reason we expand the field σ around a non-zero value σ_j , so that $\sigma = \sigma_j + \delta$ with $\delta \ll \sigma_j$. We define a new potential

$$V_k(\delta; T, \mu) = U_k(\sigma_j + \delta; T, \mu) - j(\sigma_j + \delta) \quad (33)$$

and the dimensionless quantities

$$v_k(\tilde{\delta}) = \frac{V_k(\delta; T, \mu)}{k^3 T} \quad (34)$$

$$\tilde{\delta} = \frac{\delta}{\sqrt{kT}}. \quad (35)$$

The evolution equation takes the form

$$\frac{\partial}{\partial t} v'_k(\tilde{\delta}) = -\frac{5}{2} v'_k + \frac{1}{2} \tilde{\delta} v''_k + v_3 (v'''_k) L_1^3(v''_k) + 3v_3 \left(\frac{v''_k}{\frac{\sigma_j}{\sqrt{kT}} + \tilde{\delta}} - \frac{\frac{j}{\sqrt{k^5 T}} + v'_k}{\left(\frac{\sigma_j}{\sqrt{kT}} + \tilde{\delta}\right)^2} \right) L_1^3 \left(\frac{\frac{j}{\sqrt{k^5 T}} + v'_k}{\frac{\sigma_j}{\sqrt{kT}} + \tilde{\delta}} \right), \quad (36)$$

where the primes now denote derivatives with respect to $\tilde{\delta}$.

The last term arises through the pion fluctuations. This is apparent if one considers the argument of the threshold function, which is the pion mass term $(1/\sigma)(\partial U_k/\partial\sigma)$ divided by k^2 . The term introduces explicit scale dependence in the equation. We expect the contributions that include inverse powers of k to become dominant in the infrared. The potential $u'_k(\tilde{\delta})$ could also include terms that scale with inverse powers of k . We isolate the most singular contribution by parametrizing $u'_k(\tilde{\delta})$ as

$$v'_k(\tilde{\delta}) = \tilde{v}'_k(\tilde{\delta}) + \frac{c_k}{\sqrt{k^5 T}}. \quad (37)$$

In the following we shall show that $\tilde{v}'_k(\tilde{\delta})$ can reach a scale-invariant form during the evolution, so that $\tilde{v}'_k(\tilde{\delta}) \ll j/\sqrt{k^5 T}$ for fixed $\tilde{\delta}$ and $k \rightarrow 0$. Under this assumption, we can write eq. (36) as

$$\frac{\partial}{\partial t} \tilde{v}'_k(\tilde{\delta}) = -\frac{5}{2} \tilde{v}'_k + \frac{1}{2} \tilde{\delta} \tilde{v}''_k + v_3 (\tilde{v}'''_k) L_1^3(\tilde{v}''_k) \quad (38)$$

$$\frac{d}{dk} c_k = -3v_3 \frac{(j + c_k)T}{\sigma_j^2} L_1^3 \left(\frac{j + c_k}{\sigma_j k^2} \right). \quad (39)$$

These equations have a clear physical interpretation: For sufficiently low k , the pions (the Goldstone modes) decouple from the evolution of the σ -field (the radial mode). The reason is that the pions are massive in the presence of explicit chiral symmetry breaking, with an effective mass controlled by j .

The solution of eq. (38) can reach a scale-invariant form. The only known fixed point of this equation corresponds to the Ising universality class, as only the fluctuations of the σ -field contribute to the evolution. The emergence of a critical theory around $\sigma = \sigma_j$ imposes two requirements:

- a) The first derivative of the potential around this point must vanish for $k \rightarrow 0$.
- b) The fixed point of eq. (38) must be approached during the evolution.

The solution of eqs.(38), (39) requires initial conditions. These are provided by the definition (33) for $k_T = T/\theta_2$. (As before we use $\theta_2 = 1$ for the calculations.) In particular we take

$$c_{k_T} = \frac{\partial V_{k_T}}{\partial \delta}(0; T, \mu) = \frac{\partial U_{k_T}}{\partial \sigma}(\sigma_j; T, \mu) - j \quad (40)$$

$$\tilde{v}'_{k_T} = \frac{1}{\sqrt{k_T^5 T}} \left(\frac{\partial^2 U_{k_T}}{\partial \sigma^2}(\sigma_j; T, \mu) \delta + \frac{1}{2} \frac{\partial^3 U_{k_T}}{\partial \sigma^3}(\sigma_j; T, \mu) \delta^2 + \frac{1}{6} \frac{\partial^4 U_{k_T}}{\partial \sigma^4}(\sigma_j; T, \mu) \delta^3 + \mathcal{O}(\delta^4) \right) \quad (41)$$

and neglect the higher-order terms for small δ . The first requirement for the emergence of a critical theory implies that c_{k_T} must be chosen such that the solution of eq. (39) gives $c_0 = 0$. The second requirement can be satisfied if the initial condition (41) has two properties: The term $\sim \delta^2$ (the cubic term) vanishes, and the term $\sim \delta$ (the mass term) has the appropriate critical value for the fixed point to be approached. The term $\sim \delta^3$ (the quartic coupling) need not be fine-tuned, as the Ising fixed point is characterized by one relevant parameter. For any given value of the quartic coupling, the fine-tuning of the mass term leads to the fixed point. For given j , we have three free parameters at our disposal: T , μ and the value σ_j around which we expand the potential. Therefore, we expect that the fixed point of eq. (38) can be approached for a unique choice of T , μ and σ_j . The values of these parameters mark the location of the critical endpoint on the phase diagram.

In order to determine c_0 , eq. (39) must be solved numerically. Alternatively, an analytical upper bound can be obtained through the relation

$$\ln \left(\frac{c_0 + j}{c_{k_T} + j} \right) = -3v_3 \frac{T}{\sigma_j^2} \int_{k_T}^0 dk L_1^3 \left(\frac{j + c_k}{\sigma_j k^2} \right). \quad (42)$$

The threshold function is monotonic and the maximum value of $|L_1^3(w)|$ is $|L_1^3(0)| = \sqrt{\pi}$. Thus, we obtain

$$\left| \ln \left(\frac{c_0 + j}{c_{k_T} + j} \right) \right| \leq \frac{3}{8\pi^{3/2}} \frac{T k_T}{\sigma_j^2}. \quad (43)$$

For our choice of parameters (see below) the r.h.s. is significantly smaller than 1. This implies that there is only a small difference between c_0 and c_{k_T} . As a result, the vanishing of c_0 implies $[\partial U_{k_T}/\partial \sigma](\sigma_j; T, \mu) \simeq j$, according to eq. (40).

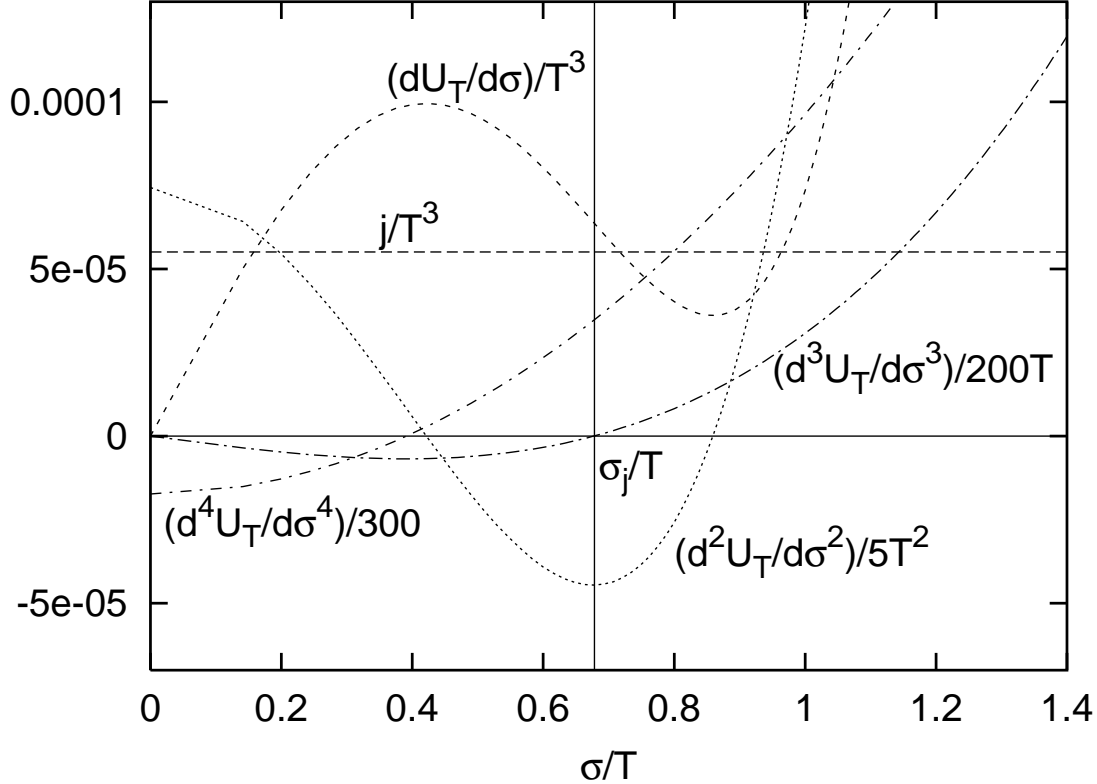


Figure 8: *Determination of the initial conditions (40), (41) for the evolution equations (38), (39).*

The determination of the initial conditions for the solution of eqs. (38), (39) is shown in fig. 8. The first four derivatives of the potential U_{k_T} at the initial scale $k_T = T$ are plotted. The point σ_j at which the third derivative vanishes is where we expect the critical theory to emerge. For the parameters of the model we have chosen ($\lambda = 0.1$, $h^2 = 2.3$, $\Lambda^2/\rho_{0R} = 1.8$), and $\mu/\sqrt{\rho_{0R}} = 0.72$, $T/\sqrt{\rho_{0R}} \simeq 0.127$, we find $\sigma_j/\sqrt{\rho_{0R}} \simeq 0.0858$. We are considering an external source $j/\rho_{0R}^{3/2} \simeq 1.12 \times 10^{-7}$. The initial value of the parameter c_{k_T} , defined in eq. (40), is $c_{k_T}/\rho_{0R}^{3/2} \simeq 1.74 \times 10^{-8}$. We observe that $[\partial U_{k_T}/\partial\sigma](\sigma_j; T, \mu)$ is close but not exactly equal to j . As a result $[\partial V_{k_T}/\partial\delta](0; T, \mu) \neq 0$.

In fig. 9 we display elements of the solution of eqs. (38), (39). We observe that the parameter $c_k = [\partial V_k/\partial\delta](0; T, \mu)$ starts from its initial value at the scale $k_T = T$ and effectively becomes zero at a scale $k/\rho_{0R}^{1/2} \simeq \exp(-6)$. The rescaled mass of the pion fields $m_\pi^2(k)/k^2 = [(j + c_k)/\sigma_j]/k^2$ becomes much larger than 1 slightly below this scale. As a result, the pions decouple completely from the evolution equation and c_k remains constant during the ensuing evolution. This guarantees that the first derivative of the potential at $k = 0$ vanishes at the point $\delta = 0$.

The solution of eq. (38) approaches a fixed point in the infrared. This is demonstrated in fig. 9 by displaying: a) the minimum $\tilde{\delta}_0 = \delta_0/\sqrt{kT}$ of the rescaled po-

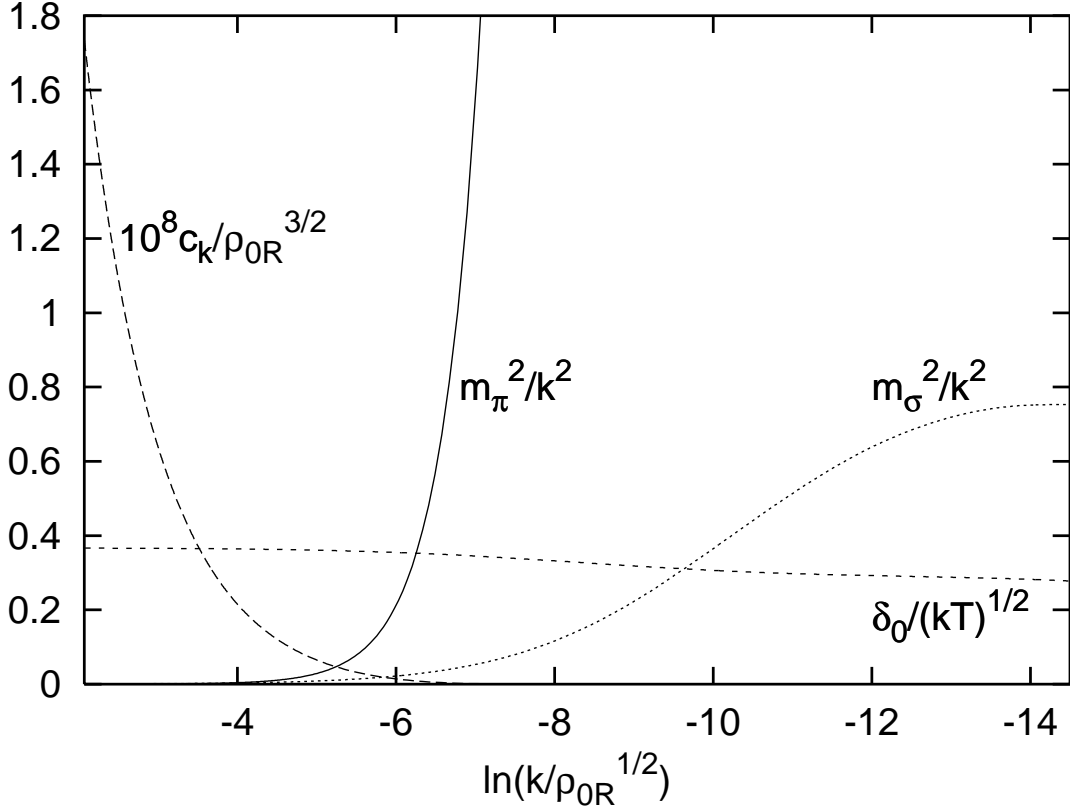


Figure 9: The evolution of: $c_k = [\partial V_k / \partial \delta](0; T, \mu)$, the rescaled σ -field and pion masses, and the minimum of $\tilde{v}_k(\tilde{\delta}) = (V_k(\delta; T, \mu) - c_k \delta) / (k^3 T)$. $\mu / \sqrt{\rho_{0R}} = 0.72$, $T / \sqrt{\rho_{0R}} \simeq 0.127$, $j / \rho_{0R}^{3/2} \simeq 1.12 \times 10^{-7}$.

tential $\tilde{v}_k(\tilde{\delta}) = (V_k(\delta; T, \mu) - c_k \delta) / (k^3 T)$; and b) the rescaled mass term $m_\sigma^2(k) / k^2 = [\partial^2 V_k / \partial \delta^2](\delta_0; T, \mu) / k^2$ of the σ -field (or the shifted δ -field) at the minimum. Both these quantities reach constant values at a scale $k / \rho_{0R}^{1/2} \simeq \exp(-14)$. The subsequent evolution is analogous to the one studied in subsection 7.1. The potential, and the various parameters derived from it, stay constant near their fixed-point values for some “time” $t = \ln(k / \rho_{0R}^{1/2})$, before finally deviating towards the symmetric or the broken phase. The renormalized theory at $k = 0$ exhibits a second-order phase transition. The parameter that has to be fine-tuned in order to go through the critical endpoint is a linear combination of T and μ .

The universality class of the fixed point is determined by the number of fields with running masses comparable or smaller than k and the symmetries of the relevant part of the action. For $k / \rho_{0R}^{1/2} \lesssim \exp(-6)$ only the σ -field fulfills this criterion. The pions have completely decoupled by the time the fixed point is approached. The scale-dependent potential $\tilde{v}(\tilde{\delta})$ has a Z_2 symmetry that is preserved by the evolution. Crucial for this conclusion is the choice of a point σ_j at which the cubic term of the potential U_{k_T} vanishes. The elimination of the pion contribution from the evolution equation (38) through the

parametrization (37) is important as well. The pion fluctuations only affect the evolution of the term linear in δ around σ_j (the parameter c_k). This term evolves to zero and stays constant after the pion decoupling. These features can be achieved for specific values of T and μ that determine the location of the critical endpoint. As a result, the endpoint belongs to the Ising universality class. This can be confirmed by calculating the critical exponents, as was done in subsection 7.1.

Before concluding this section, we should comment on the approximations employed in the study of the critical endpoint. The parametrization of eq. (37) is quite general. The derivation of the evolution equations (38), (39) made use of the crucial assumption $\tilde{v}'_k(\tilde{\delta}) \ll c_k/\sqrt{k^5 T}$. In the example we presented, the starting scale $k_T = T$ was sufficiently low for this relation to be satisfied to a good approximation during the whole evolution. We also neglected the terms higher than δ^3 in the initial condition (41) for \tilde{v}'_{k_T} . Again, this is a reasonable approximation if we are interested only in a small region around σ_j .

Going beyond these approximations in order to increase the precision of the study leads to significant technical complications. The reason is that the Z_2 symmetry of $\tilde{v}_k(\delta)$ is not guaranteed automatically if the approximations are relaxed. However, we believe that the essential conclusions remain valid. In order to have a critical theory at a point σ_j one must ensure that, at $k = 0$, the first and third derivatives of the potential are zero there. These two conditions guarantee that σ_j would be a minimum, and that no second minimum would exist in its vicinity. The appropriate choice of σ_j and the fine-tuning of a linear combination of μ and T can achieve this goal. The fine-tuning of the orthogonal combination of μ and T can be used in order to approach the fixed point that controls the critical theory. As the Ising fixed point is the only one known for the one-field theory after the pion decoupling, the resulting critical theory must be in the Ising universality class.

The demonstration that this scenario is realized, if no approximations for the potential are made, must confront non-trivial technical complications. It is difficult to keep track simultaneously of the “non-universal” part of the potential corresponding to its first and third derivatives, and the “universal” part that approaches the fixed point. The reason is that the two parts scale differently with k . Our approximations in this work simplified this task by separating the evolution of c_k from that of $\tilde{v}'(\tilde{\delta})$. The discussion of the general case merits a separate study.

9 Summary and outlook

The purpose of this study was to establish the appropriate framework for the analytical study of the QCD phase diagram, for the relatively low values of the chemical potential μ relevant for heavy-ion experiments. We employed an effective model of QCD, the linear quark-meson model. We considered only the case of two flavours, as all the expected structure of the phase diagram appears already at this level. The model is similar to the σ -model of Gell-Mann and Levy [24], with the two nucleons replaced by the u and d quarks. However, it can be extended in a straightforward manner in order to take into

account more flavours [25].

An efficient framework must involve the renormalization group, in order to provide a reliable identification of the universality classes of the various second-order phase transitions. The Wilsonian (exact) formulation of the renormalization group permits also the detailed description of weak first-order phase transitions. We employed the formalism of the effective average action [16]. We concentrated on the evolution of the non-derivative part of the action, the mesonic potential U_k , as an effective infrared cutoff k is varied. The dependence of the potential on k is described by an evolution equation that takes the form of a partial differential equation. The potential at a scale k_T equal to the temperature T serves as the initial condition. For $k = 0$ the solution becomes equal to the effective potential, from which all physical information relevant for the vacuum structure can be extracted.

We considered values of the parameters of the model that do not correspond to realistic QCD. However, they were chosen such that the discussion could be carried out with the minimum use of numerics¹. In particular, the potential at $k_T = T$ was derived analytically, using perturbation theory. Its form is determined by the potential at zero T and μ and the contributions from fluctuations with characteristic momenta larger than k_T . The fermionic fluctuations play a crucial role, as they can change the vacuum structure of the potential by generating additional minima. They decouple at scales below T , because of the effective mass developed by the fermions at non-zero temperature. As a result, the entire fermionic contributions and the mesonic contributions with momenta larger than k_T can be incorporated in the potential at k_T . The evolution below k_T is effectively three-dimensional (dimensional reduction), as only the zero-modes of the mesonic fields are light at these scales.

The other significant simplification afforded by our choice of couplings was the possibility to neglect the wavefunction renormalization of both the fermionic and mesonic fields, and the evolution of the Yukawa coupling of the meson-fermion interaction. This meant that we could use a very simple truncation of the effective average action, which involves standard kinetic terms and a general scale-dependent potential for the σ and pion fields of the mesonic sector. The evolution of the potential was determined by solving numerically a partial differential equation. As we mentioned above, the fermionic fluctuations affect only the initial condition for this equation.

The phase diagram we derived has all the expected features. For zero current quark masses, there is a line of second-order phase transitions starting on the $\mu = 0$ axis. We confirmed that they belong to the $O(4)$ universality class, by calculating universal quantities such as the critical exponents β and ν . For large μ there is a line of first-order phase transitions.

The two lines meet at a tricritical point, with specific values (μ_*, T_*) , where a second-order phase transition takes place, governed by the Gaussian fixed point. This results in mean-field behaviour, as we checked by calculating the relevant critical exponents. For

¹The parameters were also chosen such that the pattern of a second-order phase transition for $\mu = j = 0$ and increasing T and a first-order one for $T = j = 0$ and increasing μ appears. The realistic values have been shown to predict this pattern [26, 27].

μ slightly smaller than μ_* we observed universal crossover behaviour (not to be confused with the analytical crossover), as the initial influence of the Gaussian fixed point is slowly dominated by the more stable $O(4)$ fixed point near the critical temperature. For μ slightly larger than μ_* we observed very weak first-order phase transitions, for which the discontinuity in the order parameter approaches zero.

We then took into account the effects of non-zero current quark masses by introducing a source term $-j\sigma$. We discussed how the second-order phase transitions turn into an analytical crossover, while the first-order ones retain their qualitative character. We studied in detail the emergence of the critical endpoint of the line of first-order phase transitions. The pions are massive near the endpoint and we demonstrated their decoupling from the evolution equation. A second-order phase transition takes place at the endpoint, and we showed that it belongs to the Ising universality class.

The study demonstrated that it is possible to obtain a complete and detailed picture of the QCD phase diagram using an effective theory such as the quark-meson model. The renormalization group is indispensable in the process.

Realistic values for parameters of the model cannot be considered without having to rely on extensive numerical work. The most important issue concerns the value of the Yukawa coupling, which must be significantly larger than 1 for the constituent quark masses to be reproduced correctly [29]. This implies that the evolution of this coupling and the wavefunction renormalization of the fields must be taken into account. Of particular interest is the emergence of partial infrared fixed points at zero temperature and chemical potential [29, 27]. The derivation of the initial conditions for the effectively three-dimensional evolution at scales below T cannot be achieved analytically for large Yukawa couplings. However, it can be performed efficiently through the numerical integration of the appropriate evolution equations [27].

One technical issue related to the dimensional reduction of the theory at energy scales below T concerns the fermionic infrared cutoff that is used in the definition of the effective average action. A form must be devised that preserves the Lorentz structure of the kinetic term of free fermions for non-zero chemical potential, and in the same time guarantees fast decoupling of the temperature effects at low energy scales.

Finally, the strange quark can be taken into account by considering the linear quark-meson model with an $SU(3)_L \times SU(3)_R$ chiral flavour group. The increase in complexity of the resulting evolution equations is significant. However, the process can be carried out in a straightforward manner along the lines of refs. [25].

The present study has established that the linear quark-meson model is an effective theory of QCD that predicts all the expected qualitative structure of the phase diagram. The main aim of future studies along the lines highlighted above will be to determine with accuracy the location of the critical endpoint and the size of the area around it in which the critical behaviour persists. In this way, the possible effect of the endpoint on observable signatures in heavy-ion experiments will be determined quantitatively.

References

- [1] K. Rajagopal and F. Wilczek, arXiv:hep-ph/0011333.
- [2] M. Asakawa and K. Yazaki, Nucl. Phys. A **504** (1989) 668.
- [3] A. Barducci, R. Casalbuoni, S. De Curtis, R. Gatto and G. Pettini, Phys. Lett. B **231** (1989) 463; Phys. Rev. D **41** (1990) 1610; Phys. Rev. D **42** (1990) 1757; A. Barducci, R. Casalbuoni, G. Pettini and R. Gatto, Phys. Rev. D **49** (1994) 426.
- [4] S. P. Klevansky, Rev. Mod. Phys. **64** (1992) 649.
- [5] M. A. Stephanov, Phys. Rev. Lett. **76**, 4472 (1996) [arXiv:hep-lat/9604003].
- [6] M. G. Alford, K. Rajagopal and F. Wilczek, Phys. Lett. B **422** (1998) 247 [arXiv:hep-ph/9711395].
- [7] M. A. Halasz, A. D. Jackson, R. E. Shrock, M. A. Stephanov and J. J. Verbaarschot, Phys. Rev. D **58** (1998) 096007 [arXiv:hep-ph/9804290].
- [8] J. Berges and K. Rajagopal, Nucl. Phys. B **538** (1999) 215 [arXiv:hep-ph/9804233].
- [9] M. Harada and A. Shibata, Phys. Rev. D **59** (1999) 014010 [arXiv:hep-ph/9807408].
- [10] O. Kiriya, M. Maruyama and F. Takagi, Phys. Rev. D **62** (2000) 105008 [arXiv:hep-ph/0001108]; Phys. Rev. D **63** (2001) 116009 [arXiv:hep-ph/0101110].
- [11] Z. Fodor and S. D. Katz, Phys. Lett. B **534** (2002) 87 [arXiv:hep-lat/0104001]; JHEP **0203** (2002) 014 [arXiv:hep-lat/0106002].
- [12] P. de Forcrand and O. Philipsen, Nucl. Phys. B **642** (2002) 290 [arXiv:hep-lat/0205016].
- [13] C. R. Allton *et al.*, Phys. Rev. D **66** (2002) 074507 [arXiv:hep-lat/0204010].
- [14] K. G. Wilson and J. B. Kogut, Phys. Rept. **12** (1974) 75.
- [15] See, for example, the proceedings of the *2nd Conference on the Exact Renormalization Group*, Rome, Italy, 18-22 Sep 2000, and references therein.
- [16] C. Wetterich, Nucl. Phys. B **352** (1991) 529; C. Wetterich, Z. Phys. C **57** (1993) 451.
- [17] C. Wetterich, Phys. Lett. B **301** (1993) 90.
- [18] N. Tetradis and C. Wetterich, Nucl. Phys. B **422** (1994) 541 [arXiv:hep-ph/9308214].
- [19] J. Berges, N. Tetradis and C. Wetterich, Phys. Rept. **363** (2002) 223 [arXiv:hep-ph/0005122].
- [20] M. Reuter and C. Wetterich, Nucl. Phys. B **417** (1994) 181; Nucl. Phys. B **427** (1994) 291.
- [21] U. Ellwanger, Phys. Lett. B **335** (1994) 364 [arXiv:hep-th/9402077]; U. Ellwanger, M. Hirsch and A. Weber, Z. Phys. C **69** (1996) 687 [arXiv:hep-th/9506019].

- [22] M. Bonini, M. D’Attanasio and G. Marchesini, Nucl. Phys. B **437** (1995) 163 [arXiv:hep-th/9410138]; Phys. Lett. B **346** (1995) 87 [arXiv:hep-th/9412195].
- [23] T. R. Morris, Nucl. Phys. B **573** (2000) 97 [arXiv:hep-th/9910058]; JHEP **0012** (2000) 012 [arXiv:hep-th/0006064]; S. Arnone, A. Gatti and T. R. Morris, arXiv:hep-th/0209162.
- [24] M. Gell-Mann and M. Levy, Nuovo Cim. **16** (1960) 705.
- [25] D. U. Jungnickel and C. Wetterich, Phys. Rev. D **53** (1996) 5142 [arXiv:hep-ph/9505267]; Eur. Phys. J. C **1** (1998) 669 [arXiv:hep-ph/9606483]; Phys. Lett. B **389** (1996) 600 [arXiv:hep-ph/9607411].
- [26] J. Berges, D. U. Jungnickel and C. Wetterich, Eur. Phys. J. C **13** (2000) 323 [arXiv:hep-ph/9811347].
- [27] J. Berges, D. U. Jungnickel and C. Wetterich, Phys. Rev. D **59** (1999) 034010 [arXiv:hep-ph/9705474].
- [28] U. Ellwanger and C. Wetterich, Nucl. Phys. B **423** (1994) 137 [arXiv:hep-ph/9402221].
- [29] D. U. Jungnickel and C. Wetterich, arXiv:hep-ph/9610336.
- [30] Y. Nambu and G. Jona-Lasinio, Phys. Rev. **122** (1961) 345.
- [31] N. Tetradis and C. Wetterich, Nucl. Phys. B **383** (1992) 197.
- [32] N. Tetradis and C. Wetterich, Nucl. Phys. B **398** (1993) 659.
- [33] N. Tetradis, Nucl. Phys. B **488** (1997) 92 [arXiv:hep-ph/9608272].
- [34] L. Dolan and R. Jackiw, Phys. Rev. D **9** (1974) 3320.
- [35] A. Strumia and N. Tetradis, Nucl. Phys. B **542** (1999) 719 [arXiv:hep-ph/9806453]; Nucl. Phys. B **554** (1999) 697 [arXiv:hep-ph/9811438]; Nucl. Phys. B **560** (1999) 482 [arXiv:hep-ph/9904246]; JHEP **9911** (1999) 023 [arXiv:hep-ph/9904357]; A. Strumia, N. Tetradis and C. Wetterich, Phys. Lett. B **467** (1999) 279 [arXiv:hep-ph/9808263].
- [36] J. Zinn-Justin, *Quantum Field Theory and Critical Phenomena*, Oxford University Press, Oxford, 1989.
- [37] K. Rajagopal and F. Wilczek, Nucl. Phys. B **399** (1993) 395 [arXiv:hep-ph/9210253].